Deutscher Luft- und Raumfahrtkongress 2009
DocumentID: 121224

Extension of the Subsonic Doublet Lattice Method in Transonic Region using Successive Kernel Expansion

R. Thormann

Institute of Aeroelasticity, DLR, 37073 Göttingen, Germany

ABSTRACT

The Doublet Lattice Method, a panel method, is a standard tool for calculating aerodynamic forces in flutter analysis ([6], [7]). However, this method is only correct for subsonic flow conditions. The intention of this report is to investigate the successive kernel expansion method (SKEM), a method from literature, which promise a successful extension of the DLM into transonic regions. The kernel function is expanded as a Taylor series with respect to the reduced frequency about $\omega^* = 0$. The first element is representing the quasi steady part of the solution and is corrected by the difference of two steady CFD (Computational Fluid Dynamics) calculations with different angles of attack.
The main advantage over other so called reduced order methods is that no numerical simulations in the flow field are required. Pressure differences are directly calculated at the surface of the wing or aircraft. In contrast to the Transonic Doublet-Lattice Method (TDLM), in which terms are added obtained from one steady CFD simulation[9], SKEM extrapolates from a quasi steady solution at $\omega^* = 0$ to the unsteady pressure differences.
In [5] the method is only validated for very low frequencies and only two Taylor coefficients are taken into consideration. This restriction could be successfully disbanded by higher Taylor expansion. The Taylor series is computed using automatic differentiation techniques. Furthermore convergence properties are analyzed and an improved SKEM (iSKEM) is developed. Moreover the method is compared to nonlinear unsteady simulations in the time domain using the DLR TAU-Code and to measurement data of the AGARD LANN wing. Computed transonic cases include Euler calculations for various frequencies and RANS calculations with separation and inverse shock movement.

1. INTRODUCTION

For flutter analysis, unsteady aerodynamic forces of harmonic oscillating airfoils are needed for many mach numbers and reduced frequencies. In the industrial process the Doublet-Lattice Method is a standard tool for calculating unsteady aerodynamics [6]. It is an integral equation method that determines the time depend pressure differences between e.g. the lower and upper wing skin. However DLM is a compressible subsonic method which uses isentropic change of state and so it is incorrect for transonic flow conditions. In this region the nonlinear flow differential equations cannot easily be transformed in a DLM formulation, so time-consuming CFD (Computational Fluid Dynamic) methods solving the partial differential equations directly have to be applied.
In this paper a method is investigated to correct the DLM results with CFD calculations: The Successive Kernel Expansion Method (SKEM). The Doublet-Lattice kernel function is expanded as Taylor series with respect to the reduced frequency ω^* about the quasi steady state. The first element is corrected by the difference of two steady CFD solutions at different states of the oscillation, with different angles of attack [5].

After a short description of the Successive Kernel Expansion method, convergence properties and computational complexities are determined and an improved SKEM (iSKEM) is developed. Finally the method is compared to nonlinear unsteady simulations in the time domain using the TAU-Code and with measuring data.

2. SUCCESSIVE KERNEL EXPANSION METHOD (SKEM)

In this chapter a short overview is given on the Successive Kernel Expansion Method (SKEM). Starting point is the integral equation of the DLM

$$w = \frac{1}{8\pi} \iint_A \Delta c_p K(x-\xi, y-\eta, 0)\, d\xi\, d\eta \tag{1}$$

with upwind w and the kernel function K. All terms are now expanded as Taylor series with respect to the reduced frequency ω^*. So the k-th Taylor coefficient of the upwind w can be expressed as:

$$w^{(k)} = \frac{1}{8\pi} \iint_A \sum_{j=0}^{k} \Delta c_p^{(j)} K^{(k-j)}(x-\eta, y-\xi, 0) d\eta d\xi \tag{2}$$

and with the same steps as in the classic DLM this equation can be reduced to:

$$\begin{aligned} w^{(k)} &= \frac{1}{8\pi} \sum_{j=0}^{k} \Delta\xi^i_{\frac{1}{2}} \Delta c_p^{(j)} \int_{-L}^{L} K^{(k-j)}(y^j - \sin(\lambda)\xi^i)\, d\xi^i \\ &= \sum_{j=0}^{k} AIC^{(j)}\, \Delta c_p^{(k-j)} \end{aligned} \tag{3}$$

Finally, the resulting linear system has to be solved for the unknown $\Delta c_p^{(k)}$:

$$[AIC]^{(0)}\ \Delta c_p^{(k)} = w^{(k)} - \sum_{j=0}^{k-1} AIC^{(j)}\, \Delta c_p^{(k-j)} \tag{4}$$

$[AIC]^{(0)}$ is the AIC matrix for the reduced frequency $\omega^* = 0$ and represents the quasi steady part. This matrix will be corrected by two steady CFD results:

$$w^{(0)} = AIC^{(0)}\,\Delta c_p^{(0)} \text{ (DLM theories)} \tag{5}$$
$$= C\,AIC_0\,\Delta c_p^{(0),\,given}$$

$$\Delta c_p^{(0),\,given} = \frac{\Delta c_p^{CFD}(\alpha_1) - \Delta c_p^{CFD}(\alpha_2)}{\alpha_1 - \alpha_2} \tag{6}$$

with the correction matrix C. Equation (4) can be solved efficiently by L-U factorisation of $C \cdot [AIC]^{(0)}$.

3. Improved Successive Kernel Expansion Method (ISKEM)

In [5] only two Taylor coefficients are taken into account. In this chapter this restriction will be disbanded and a short complexity analysis will be performed.

3.1. Computation of the Taylor series

Calculating the Taylor series of the kernel function analytically is difficult, results in high implementation costs and make the code more error-prone. A particular challenge is the computation of the integral $I_1 = \int_{u_1}^{\infty} \frac{e^{i\omega^* u}}{(1+u^2)^{\frac{3}{2}}}\,du$. Figure 1 confirms that the Laschka approximation leads to very small convergence radius of the Taylor series.

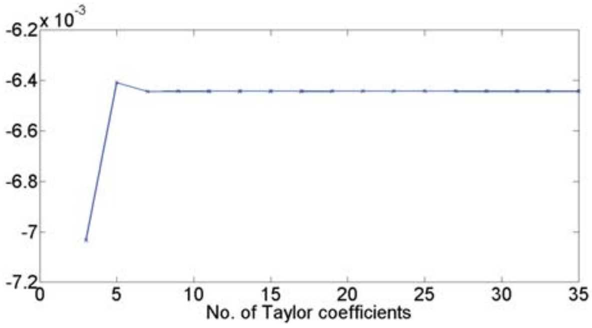

(a) imag. part of I_1, Gaussian quadrature

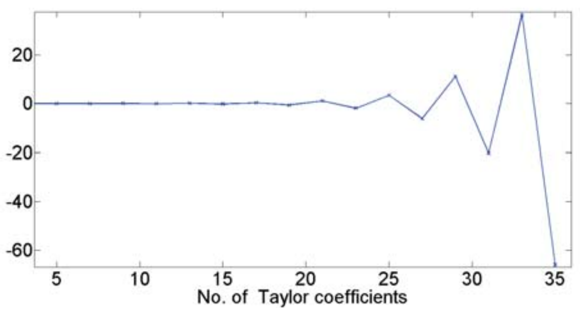

(b) imag. part of I_1, Laschka approximation

Fig. 1: convergence comparison of computing the Taylor series of imag(I_1)

Evaluating the integral analytically causes diverging integrals for $n \geq 2$:

$$\frac{d^n}{d(\omega^*)^n} \int_{u_1}^{\infty} \frac{e^{i\omega^* u}}{(1+u^2)^{\frac{3}{2}}}\,du\bigg|_{\omega^*=0} = \int_{u_1}^{\infty} \frac{d^n}{d(\omega^*)^n} \frac{e^{i\omega^* u}}{(1+u^2)^{\frac{3}{2}}}\,du\bigg|_{\omega^*=0}$$
$$= \int_{u_1}^{\infty} \frac{u^n e^{i\omega^* u}}{(1+u^2)^{\frac{3}{2}}}\,du\bigg|_{\omega^*=0} = \int_{u_1}^{\infty} \frac{u^n}{(1+u^2)^{\frac{3}{2}}}\,du$$

Hence, the integral is computed using a Gaussian quadrature which make it very hard to calculate the Taylor series symbolically. For this reason the Taylor series is computed automatically using Taylor arithmetic.

For evaluating Taylor series automatically, a new datatype for holding the Taylor coefficients was defined and all necessary operators and functions were overloaded. Real and imaginary part are computed separately. For more details about Taylor arithmetic's look at [3],[4], [8].

Of course, only finite Taylor series can be considered, hence remainder terms exists. It is easy to show, that for each operation on Taylor series needed for the kernel function expansion, the "output" Taylor series converges if the "input" Taylor series are converged.

3.2. Computational Complexity

The computational complexity of the automatic computation of Taylor series for the addition of two series is:

$$OPS(z_0,\ldots,z_d) = d\;OPS(z_0 = F(x_0))$$

The product of two Taylor series is a convolution sum and so the complexity becomes:

$$OPS(z_0,\ldots,z_d) = d^2\;OPS(z_0 = F(x_0))$$

The Taylor coefficients of sinus and cosines terms are computed directly and so the complexity is linear in the number of Taylor coefficients. The efficient number of Taylor coefficient may be halved by avoiding recomputing zeros (every second Taylor coefficient of sinus and cosines is zero).

$$OPS(z_0,\ldots,z_d) = \frac{d}{2}\;OPS(z_0 = F(x_0))$$

In SKEM, for computing Δc_p one has to:

- solve $N+1$ linear systems of equations
- add $1 + \frac{N(N-1)}{2}$ vectors
- calculate $\frac{N(N+1)}{2}$ matrix-vector products

Thus the computational costs for computing Δc_p increase with $O(N^2)$, where N is the number of regarded Taylor coefficients. If you expand the AIC matrix as Taylor series and merge the series again after correcting the quasi steady part with CFD results (iSKEM):

$$tAIC = C \cdot AIC^{(0)} + \sum_{k=1}^{N} AIC^{(k)} (i\omega^*)^k,$$

the complexity is only $O(N)$. Afterwards, the linear system $w = tAIC\,\Delta c_p$ must be solved as in classic DLM. The next chapter will show that this approach leads to better convergence.

4. NUMERICAL EXPERIMENTS

The AGARD LANN wing [2] is used for validation because of the complex shock structure and existing experimental data. In each test case pitching motions about the 62% chord axis were investigated. The CFD correction for DLM was calculated from a steady simulation at mean and maximal angle of attack.

First of all Euler computations were performed with reduced frequencies 0.1, 0.5 and 1.0 in order to study general convergence properties. The consistency of results was controlled at three cuts (Fig.2) and on the global lift coefficient c_L.

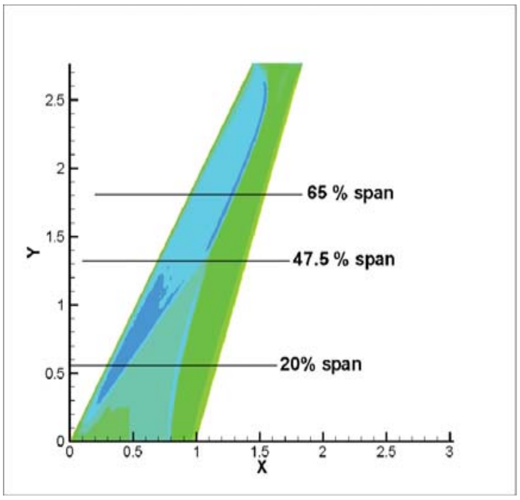

Fig. 2: position of cuts, steady cp (Euler) at AoA=0.6°

4.1. Convergence Studies

In this section SKEM and iSKEM will be analysed regarding the convergence of the Taylor series. In all cases the external steady input data from the CFD solver TAU are computed at an angle of attack of $0.6°$ and $0.8°$ to simulate a pitching motion about $0.6°$ with an amplitude of $0.2°$. The convergence properties are studied on a 30×30 Doublet Lattice grid (Fig.3).

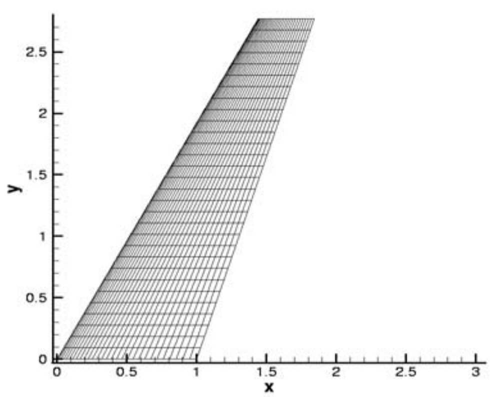

Fig. 3: Doublet-Lattice grid with 30 spanwise and chordwise boxes

Table 1: comparison of the global lift coefficient of DLM and **SKEM without** CFD correction

ω^*	DLM		SKEM	
	c_L^{real}	c_L^{imag}	c_L^{real}	c_L^{imag}
0.1	6.09800	-0.21305	6.08090	-0.22004
0.5	5.18891	0.13460	5.21377	0.09159
1.0	4.80541	1.35127	4.98068	1.15864

Table 2: comparison of the global lift coefficient of DLM and **iSKEM without** CFD correction

ω^*	DLM		iSKEM	
	c_L^{real}	c_L^{imag}	c_L^{real}	c_L^{imag}
0.1	6.09800	-0.21305	6.08089	-0.22004
0.5	5.18891	0.13460	5.16204	0.12964
1.0	4.80541	1.35127	4.77691	1.34867

An overview of the c_L values is given in table 1 and 2: iSKEM shows better results than SKEM for higher frequencies, it can reproduce the DLM results. In figures 4, 5 and 6 the convergence of c_L with CFD correction is shown.

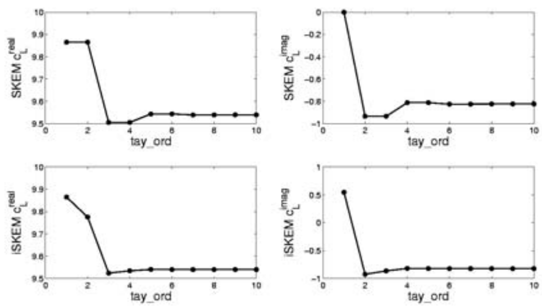

Fig. 4: convergence of c_L for $\omega^* = 0.1$

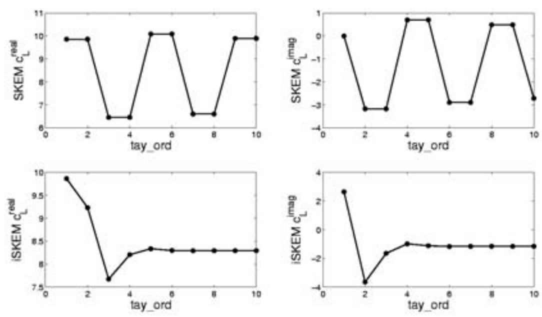

Fig. 5: convergence of c_L for $\omega^* = 0.5$

The upper two diagram's represent the unsteady lift coefficient if Δc_p is computed successively (SKEM). In the lower diagram's the convergence behavior of c_L is shown if the first Taylor coefficient of the AIC matrix is CFD corrected and afterwards the series is added together (iSKEM = improved Successive Kernel Expansion).

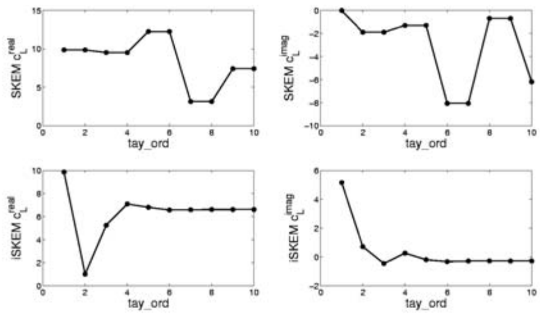

Fig. 6: convergence of c_L for $\omega^* = 1.0$

Generally it is sufficient to consider ten Taylor coefficients. In most cases the series even converges after six coefficients. For low reduced frequencies both methods are converging after a few coefficients. The behavior of SKEM is changing with increasing frequency: for $\omega^* = 0.5$ and 1.0 the Taylor series do not converge anymore. This can be seen without CFD correction, too (Tab. 1). However when using iSKEM the Taylor series converges independent from the reduced frequency.

In SKEM all three terms of $w = AIC\, \Delta c_p$ are expanded as Taylor series and the individual coefficients are calculated iteratively. Both Taylor series of w and AIC are converging. Whereas it is valid, that if the Taylor series of both factors of a product are converging the product itself converges, the opposite is usually not valid. The Taylor series of Δc_p corresponds to the Taylor series of $AIC^{-1}w$. In the elements of AIC^{-1} the independent variable ω^* appears in the denominator. From this it follows that the Taylor series has a very small convergence radius. In contrast, iSKEM requires only the convergence of the Taylor series of the AIC matrix, which is given for any reduced frequency.

4.2. Validation for Euler simulations

After the convergence of iSKEM is proven the method will now be validated with CFD simulations in the time domain using the non-linear solver TAU. Because of the lower computational costs with respect to RANS calculations, first some unsteady Euler simulations are accomplished with various reduced frequencies and compared to iSKEM results.
In all simulations the mean angle of attack was $0.6°$ and the amplitude was $0.2°$. In the following figures the complex Δc_p calculated from a Fourier transformation are compared on local cuts.

Table 3: legend for pressure characteristics

red line	Δc_p from unsteady non-linear TAU simulation
green line	Δc_p from iSKEM

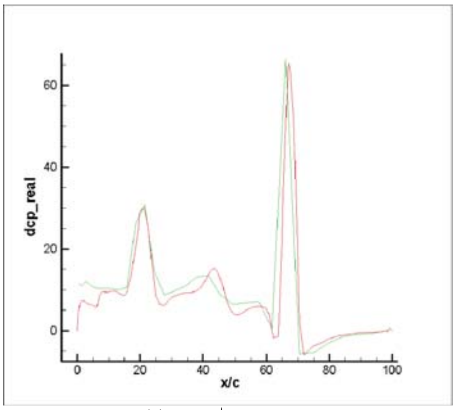

(a) Δc_p^{real} 20% span

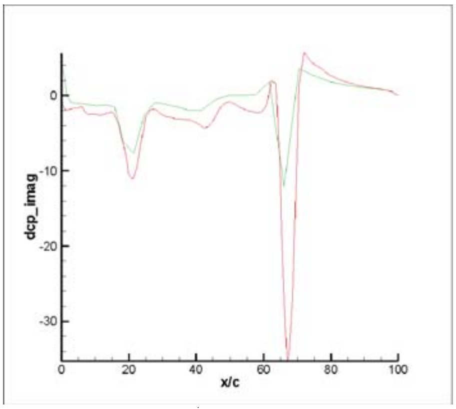

(b) Δc_p^{imag} 20% span

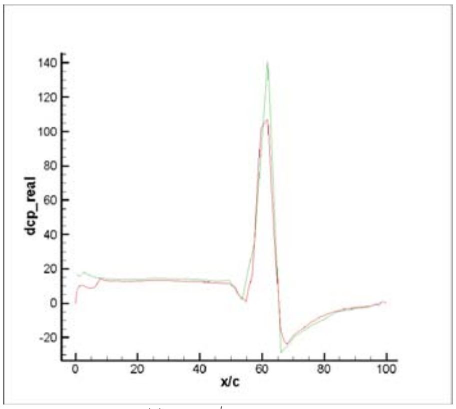

(c) Δc_p^{real} 65% span

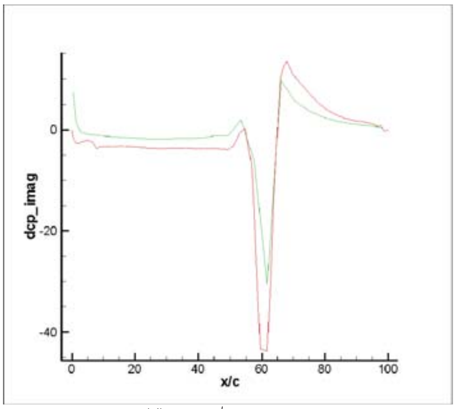

(d) Δc_p^{real} 65% span

Fig. 7: unsteady Δc_p for $\omega^* = 0.1$

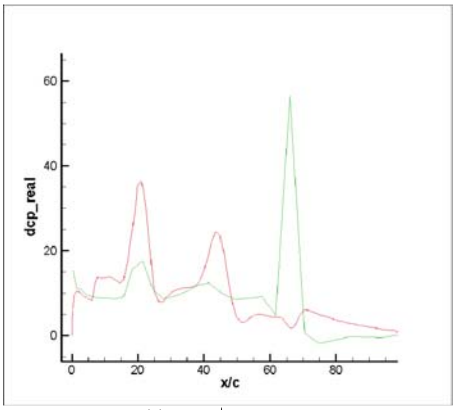

(a) Δc_p^{real} 20% span

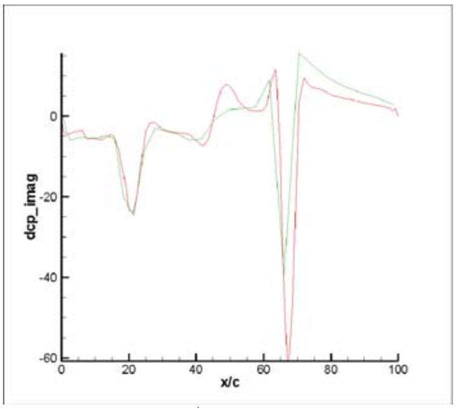

(b) Δc_p^{imag} 20% span

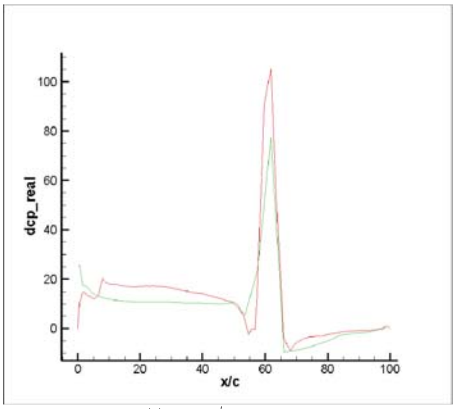

(c) Δc_p^{real} 65% span

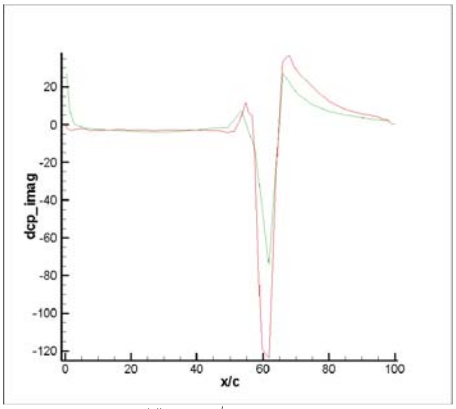

(d) Δc_p^{real} 65% span

Fig. 8: unsteady Δc_p for $\omega^* = 0.5$

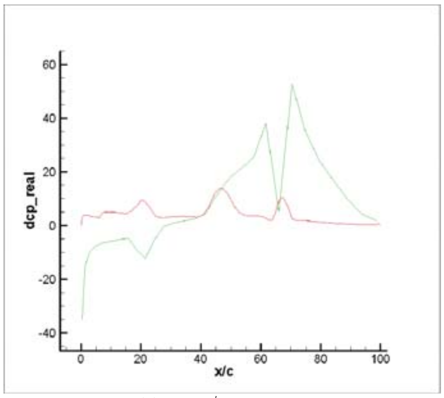

(a) Δc_p^{real} 20% span

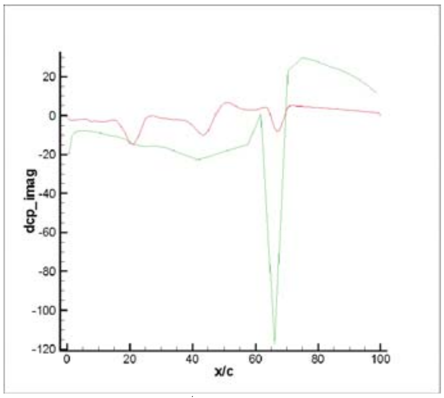

(b) Δc_p^{imag} 20% span

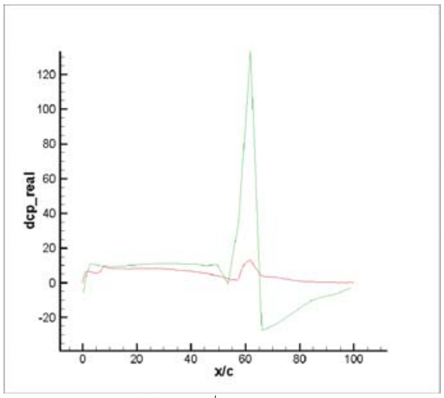

(c) Δc_p^{real} 65% span

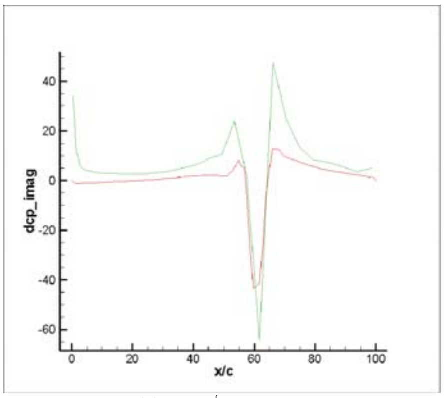

(d) Δc_p^{real} 65% span

Fig. 9: unsteady Δc_p for $\omega^* = 1.0$

The curve characteristics agree very well for low frequencies (Fig. 7). There are some small differences in the level, but they are decaying when moving towards the tip. In this region, the shock structure is simpler, no double shock system exist.
The iSKEM results agree well until $\omega^* = 0.3$. The level differences are higher at $\omega^* = 0.5$ and for the inner cuts the shock positions agree not very well (Fig. 8).
The curve characteristics of iSKEM and TAU do not agree anymore for even higher frequencies, e.g. $\omega^* = 1.0$ (Fig. 9), although iSKEM is converging and without CFD correction reproduces the DLM results. This is due to the transonic flow conditions: the pressure curves have little similarities with the quasi-steady solution at $\omega^* = 0$. Therefore, the influence of the reduced frequency is too strong and iSKEM cannot reproduce the CFD results.

4.3. Validation for RANS simulations

In the following, wind tunnel test cases are simulated with DLR TAU code to validate iSKEM for flow involving friction.
The first test case CT5 describes a pitching motion about a mean angle of attack $\alpha_0 = 0.6°$ with amplitude $\bar{\alpha} = 0.25°$, reduced frequency $\omega^* = 0.204$ and Reynolds number $Re = 7.3 \cdot 10^6$.
The second test case CT9 is a pitching motion as well, but with higher mean angle of attack: $\alpha_0 = 2.6°$. The other parameters are almost the same. The CFD correction for iSKEM is calculated from steady computations at $\alpha_0 = 0.6$ and 0.85 for CT5 and at $\alpha_0 = 2.6$ and 2.85 for CT9.

The pressure characteristics of iSKEM without CFD correction reproduced the DLM solution and are not shown here. The steady experimental data do not perfectly agree with TAU (Fig. 10), especially for CT9 where shock separation occurs. A reason for this could be that the grid is too coarse in the shock regions. From this, it cannot be extrapolated that iSKEM will match with the experiment, but it should agree well with the URANS TAU solutions.

Table 4: legend

red line	nonlinear TAU
green line	iSKEM
black line	experiment

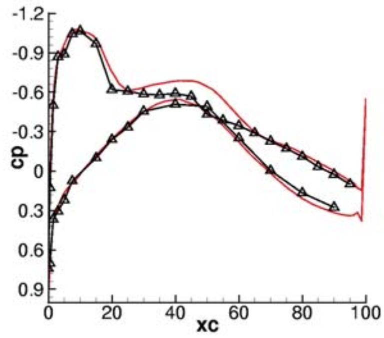

(a) CT5: Δc_p 20% span

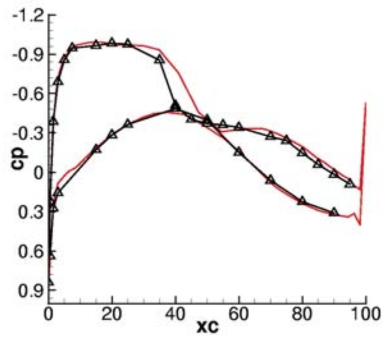

(b) CT5: Δc_p 65% span

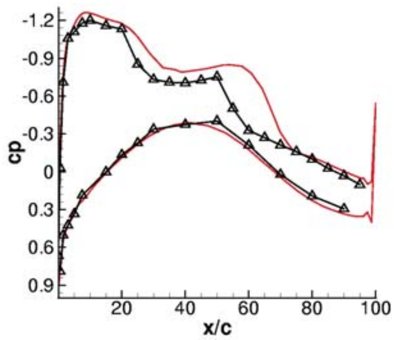

(c) CT9: Δc_p 20% span

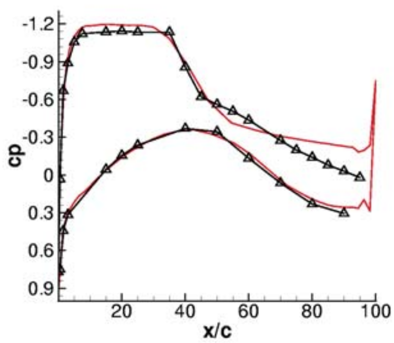

(d) CT9: Δc_p 65% span

Fig. 10: steady Δc_p for CT5 and CT9

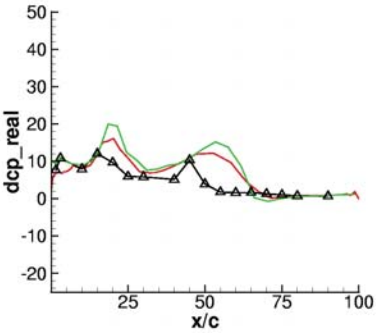

(a) Δc_p^{real} 20% span

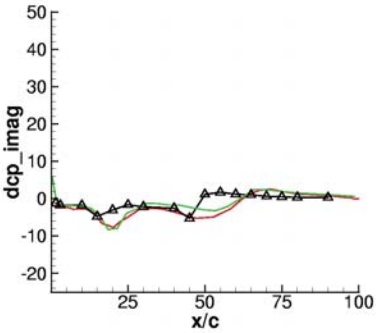

(b) Δc_p^{imag} 20% span

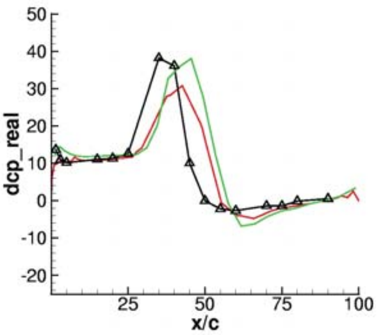

(c) Δc_p^{real} 65% span

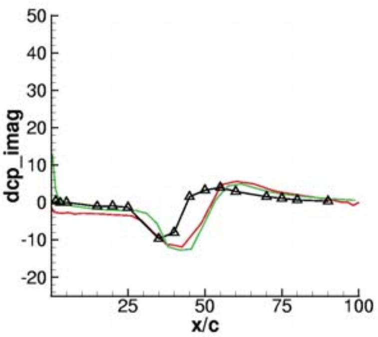

(d) Δc_p^{imag} 65% span

Fig. 11: unsteady Δc_p for CT5

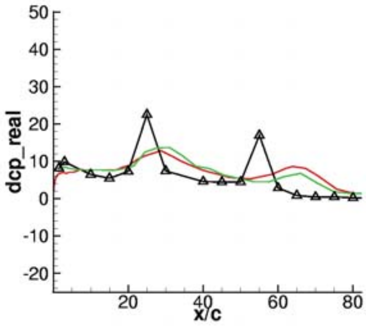

(a) Δc_p^{real} 20% span

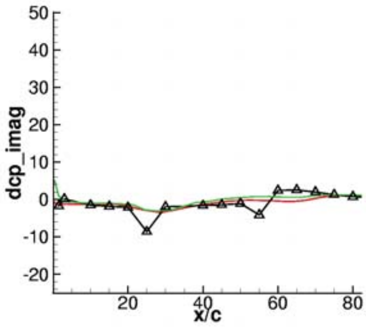

(b) Δc_p^{imag} 20% span

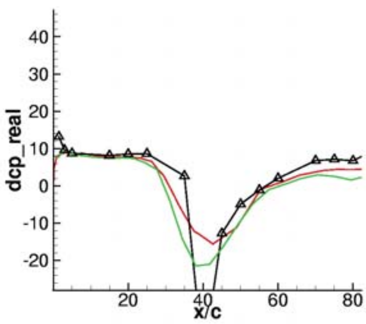

(c) Δc_p^{real} 65% span

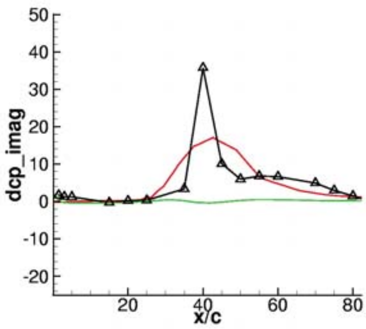

(d) Δc_p^{imag} 65% span

Fig. 12: unsteady Δc_p for CT9

The results from iSKEM agree very well with the CFD data for CT5, Fig. 11 (only small differences in the level).

The CT9 is a bit more complicated. The supersonic region is stronger due to the higher angle of attack and the flow separates. These are the reasons why the agreement of iSKEM and CFD is worse.
The separation causes an inverse shock motion: when the angle of attack increases the shock moves stream up instead of moving stream down, because the separation region increases.
As long as the flow is still attached the results for CT9 agree well. This is the case in the inner region of the wing (Fig. 12(a) and 12(b)). In the outer region the flow separates and inverse shock motion appears. There are big differences between iSKEM and TAU. The inverse shock motion, indicated by a change in sign of real and imaginary part compared to CT5, is also in trend reflected in the iSKEM results.

The flow separation can also be seen in the steady case, at angle of attack $\alpha_0 = 2.85$. In the contour plot of the x-velocity of the flow (Fig:13(a) and 13(b)) this is indicated by a local region with upstream flow and a strong increase in boundary layer thickness.

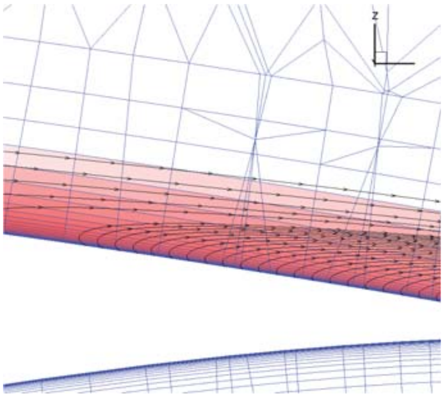

(a) streamtraces and contour of x-velocity

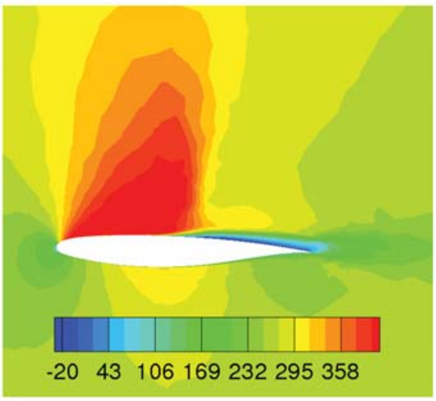

(b) contour of x-velocity

Fig. 13: CT9: steady separation at 47.5% span and $AoA = 2.85°$

Overall the LANN test case is not a difficult case for iSKEM, because a reduced frequency about 0.2 is still low. The influence of the additional unsteady terms from the DLM compared to the quasi-steady CFD input Δc_p^{given} is relatively small in the real part. iSKEM accomplishes the main effect in the imaginary part that is by definition zero in the CFD input.
Figures 14 and 15 point out the considerable improvement in unsteady loads compared to the DLM, but also that the error becomes too large after $\omega^* = 0.3$.

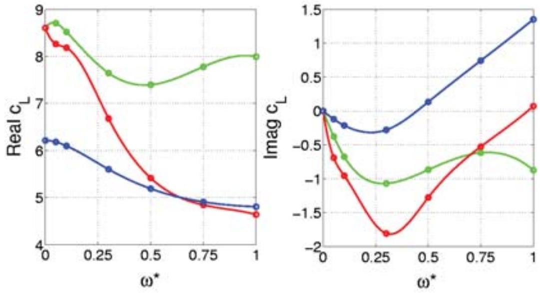

Fig. 14: c_L progression over ω^* for CT5

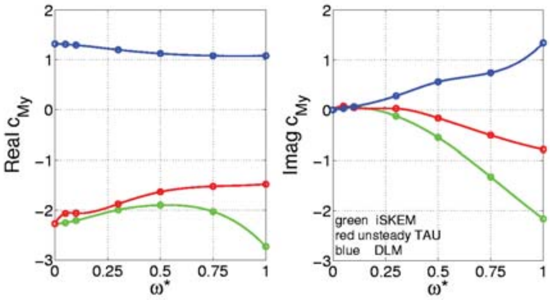

Fig. 15: c_{My} progression over ω^* for CT5

4.4. CPU Time Comparison

Table 5: CPU times of iSKEM for calculating the AIC matrix and the CFD correction

No. DLM Boxes	No. Taylor coeff.	mean CPU time(sec)
400	6	202.86
400	8	223.32
400	10	234.91
600	6	469.03
600	8	542.63
600	10	552.44
900	6	1022.52
900	8	1093.69
900	10	1159.4

The computation of the AIC matrix on an Intel Xeon CPU with 2.66 Ghz on a fine grid (30×30 boxes) of a clean planar wing takes about 20 minutes. Afterwards, only a linear system of equations has to be solved, with nearly no costs using a preceding L-U factorisation.
A steady RANS simulation with the DLR TAU code lasts in contrast about 3 hours to converge the residuum about 6 orders of magnitude on 12 Intel Xeon CPU with 3 Ghz and the unsteady simulation for CT9 lasted 2 days on 24 AMD Barcelona

CPU.
Compared to the classic DLM, which takes only half a minute for the same problem, 20 minutes are a great increase in CPU time. Main reasons for the increment are the automatic Taylor expansion and the numerical integration in the kernel function (in the classic DLM the integrals are solved via Laschka approximation [1]).

5. CONCLUSIONS AND FURTHER WORK

The Successive Kernel Expansion Method (SKEM) was analysed and an improved method (iSKEM) was derived, to extend the subsonic Doublet Lattice Method into transonic regions. Therefore, Taylor arithmetic's were implemented to calculate the Taylor coefficients of the kernel function automatically. It was shown that the iterative computation of the Taylor series of Δc_p induce small convergence radiuses. In contrast to SKEM the approach in iSKEM leads to convergence for any reduced frequency. It is sufficient to correct the first, quasi-steady Taylor coefficient of the AIC matrix with two steady CFD results, adding the coefficients together again and solve the linear system to get the unsteady Δc_p.
It is important to note that this CFD correction can only be made with modes that involve a change of the angle of attack. Otherwise the quasi-steady solution is zero.

iSKEM was validated with unsteady non-linear CFD simulations in the time domain in comparison to the example of the LANN wing. For low frequencies iSKEM delivers good results except small differences in the level, especially in the double shock region. These differences are growing with increasing frequency. The pressure progressions of iSKEM and TAU at $\omega^* = 1.0$ do not agree anymore. The reason for this can be found in the modeling. The unsteady pressures for high frequencies have no similarities with the quasi-steady solution at $\omega^* = 0$. The unsteady correction terms of the subsonic DLM, Taylor coefficients of higher order, cannot reproduce the effects.
iSKEM delivers good results for flow involving friction, too, as long as there is no separation or inverse shock motion involved. These characteristic's iSKEM can only adumbrate.
The computational costs of iSKEM are higher compared to DLM but are still low compared to full non-linear CFD simulations in the time domain.

Overall the results in the unsteady global forces are significantly better predicted by iSKEM compared to the classic subsonic DLM by only little more computational complexity.

REFERENCES

[1] Blair, M. : *A Compilation Of The Mathematics Leading To The Doublet Lattice Method*, 1992

[2] Bland, S. R.: *AGARD Three-Dimensional Aeroelastic Configurations*, AGARD Advisory Report No. 167, 1982

[3] Blomquist, F., Hofschuster, W., Krämer, W.:*Real and Complex Taylor Arithmetic in C-XSC*, Bergische Universität Wuppertal, www.math.uni-wuppertal.de/wrswt/literatur.html, 02.10.2008

[4] Griewank, A: *Evaluating Derivatives: Principles and Techniques of Algorithmic Differentiation*, SIAM, Philadelphia 2000

[5] Chen P.C., Silva, R.G.A., Liu, D.D.: *Transonic AIC Weighting Method using Successive Kernel Expansion*, AIAA 2005-1991, 2005

[6] Försching, H. W.:*Grundlagen der Aeroelastik*, Springer-Verlag, 1974

[7] Rodden W.P., Giesing J.P., Kalman T.P.:*Refinement of the Nonplanar Aspects of the Subsonic Doublet-Lattice Lifting Surface Method*, J. Aircraft Vol. 9 No. 1, Januar 1972

[8] Thormann, Reik: *Erweiterung der subsonsichen Doublet Lattice Methode in die Transsonik mittels sukzessiver Kernentwicklung*, Forschungsbericht, DLR Göttingen, Institute of Aeroelasticity, 2009

[9] Lu, S., Voss R.: *TDLM - A Transonic Doublet Lattice Method for 3D-potential Unsteady Transonic Flow Calculation and its Application to Transonic Flutterprediction*, Proceedings: Forum International Aeroelasticite et Dynamique de Structures, Vol.1, Strasbourg, 1993